LBL-35261
Preprint

Lawrence Berkeley Laboratory
UNIVERSITY OF CALIFORNIA

CHEMICAL SCIENCES DIVISION

Submitted to C.N.R. Rao Festschrift
Special Issue of the Journal of Physical Chemistry

Final-State Effects in the Angle-Resolved Photoemission Extended Fine Structure of c(2×2)S/Ni(001)

W.R.A. Huff, Y. Zheng, Z. Hussain, and D.A. Shirley

February 1994

LOAN COPY
Circulates
for 4 weeks
Bldg. 50 Library.
LBL-35261
Copy 2

Prepared for the U.S. Department of Energy under Contract Number DE-AC03-76SF00098

DISCLAIMER

This document was prepared as an account of work sponsored by the United States Government. While this document is believed to contain correct information, neither the United States Government nor any agency thereof, nor the Regents of the University of California, nor any of their employees, makes any warranty, express or implied, or assumes any legal responsibility for the accuracy, completeness, or usefulness of any information, apparatus, product, or process disclosed, or represents that its use would not infringe privately owned rights. Reference herein to any specific commercial product, process, or service by its trade name, trademark, manufacturer, or otherwise, does not necessarily constitute or imply its endorsement, recommendation, or favoring by the United States Government or any agency thereof, or the Regents of the University of California. The views and opinions of authors expressed herein do not necessarily state or reflect those of the United States Government or any agency thereof or the Regents of the University of California.

LBL-35261

Final-State Effects in the Angle-Resolved Photoemission Extended Fine Structure of c(2×2)S/Ni(001)

W.R.A. Huff,[a] Y. Zheng,[a,b] Z. Hussain,[c] and D.A. Shirley[b]

[a]Chemical Sciences Division
Lawrence Berkeley Laboratory
University of California
Berkeley, CA 94720

[b]Departments of Chemistry and Physics
Pennsylvania State University
University Park, PA 16802

[c]Accelerator and Fusion Research Division
Lawrence Berkeley Laboratory
University of California
Berkeley, CA 94720

February 1994

This work was supported by the Director, Office of Energy Research, Office of Basic Energy Sciences, Chemical Sciences Division of the U.S. Department of Energy under Contract No. DE-AC03-76SF00098.

Final-State Effects in the Angle-Resolved Photoemission Extended Fine Structure of c(2x2)S/Ni(001)

W.R.A. Huff,[a] Y. Zheng,[a,b] Z. Hussain,[c] and D.A. Shirley[b]

[a]*Chemical Sciences Division, Lawrence Berkeley Laboratory, University of California, Berkeley, CA 94720*

[b]*Departments of Chemistry and Physics, Pennsylvania State University, University Park, PA 16802*

[c]*Accelerator and Fusion Research Division, Lawrence Berkeley Laboratory, University of California, Berkeley, CA 94720*

ABSTRACT

Final-state effects on angle-resolved photoemission extended fine structure (ARPEFS) $\chi(k)$ curves were studied using previously published normal-emission experimental data from the S 1*s* and S 2*p* core levels of c(2x2)S/Ni(001). The two $\chi(k)$ curves appeared to be approximately 180° out of phase as predicted by Tong and Tang. However, in contrast to the expectations based on plane-wave theory, the Fourier transforms of the experimental S 1*s* and S 2*p* data sets are quite different, with a Generalized Ramsauer-Townsend splitting present in the 1*s* but not in the 2*p* data. Multiple-scattering spherical-wave calculations were carried out to study the final-state effects. Based on the calculations, an approximate method for analyzing ARPEFS data from a non-s initial-state using only the higher-ℓ partial wave was proposed and successfully tested with the experimental S 2*p* ARPEFS data.

PACS numbers: 61.14.-x,68.35.Bs,79.60.Dp

Angle-resolved photoemission extended fine structure (ARPEFS), in which angle-resolved core-level photoemission intensities from surface atoms are measured over a wide photoelectron kinetic-energy range, is a proven technique for surface/interface structure determination.[1-5] In the past few years, ARPEFS has been used successfully to study the local atomic structure around the adsorbate atoms and the adsorbate-induced relaxation of the substrates.[6-13] In these studies, Fourier transform (FT) analyses yielded qualitative and semi-quantitative surface structural information. The peaks in the ARPEFS-FT spectrum correspond to path-length differences (PLDs) between the direct wave and single-scattered waves, plus a phase shift. Additionally, multiple-scattering spherical-wave (MSSW) analyses of ARPEFS $\chi(k)$ data yielded quantitative surface structures.

Most of the above ARPEFS studies were based on photoemission data from atomic *s* core-level initial states, for which the selection rule $\Delta\ell_i = \pm 1$ gives a *p*-wave final state. Our experience with ARPEFS data from non-*s* initial states, and their FTs, is very limited, however. For non-*s* initial states ($\ell_i \neq 0$), the photoelectron final state is made up of partial waves with orbital quantum numbers $\ell_i + 1$ and $\ell_i - 1$, and a phase relationship between them which leads to interference between the two partial waves. The partial wave transition matrix elements and the phase angle are in general energy-dependent. Despite these complications, there are a number of interesting experimental situations for which ARPEFS studies on a non-*s* initial state may confer some advantage. For this reason, as well as general curiosity, we decided to look more carefully into a comparison of the existing data on the c(2x2)S/Ni(001) system. Two unanticipated results emerged. First, the Fourier transforms of the two data sets differed substantially, with a peak being split by the Generalized Ramsauer-Townsend Effect in one data set but not in the other. Second, the dominance of the $\ell_i + 1$

partial wave in the final state is so strong that the data could be analyzed with very good accuracy by using this wave alone, ignoring the $\ell_i - 1$ wave.

Tong and Tang[8] reported a theoretical study of the effect of final-state symmetry on normal photoelectron diffraction data, based on calculations of backscattering from sub-surface crystal layers. They derived the factor $(-1)^{\ell_i+1}$ to describe the phase relationship of ARPEFS $\chi(k)$ data from an arbitrary initial state. According to this factor, the ARPEFS $\chi(k)$ curves for initial states of odd ℓ_i are predicted to be 180° out of phase relative to those for initial states of even ℓ_i. Furthermore, their calculations showed for c(2x2)S/Ni(001) that, in their layer-scattering model, the ARPEFS $\chi(k)$ curves from different initial states would have the same frequencies, and the ARPEFS-FTs would therefore have the same peak positions. Tang[8] later examined the data, found quite good agreement, and concluded that these predictions were borne out.

In the present work, we have re-investigated this issue in more detail, using the same experimental S 1*s* and S 2*p* ARPEFS data from c(2x2)S/Ni(001). Both data sets had been measured normal to the crystal surface plane because in the early work the "normal photoelectron diffraction," or NPD, mode was regarded as special, consistent with the picture of backscattering off crystal planes rather than atoms. The photon polarization vectors were oriented 30° and 35° off the surface normal toward the [011] direction.[9,10]

Figure 1a compares these two ARPEFS data sets. The experimental S 1*s* and S 2*p* ARPEFS $\chi(k)$ curves are indeed approximately 180° out of phase as predicted by Tang and Tong. Again we note that this prediction was made in the context of a scattering model of plane waves backscattering from sub-surface crystal layers. The FT of a normal-emission curve was regarded as yielding the distances to these layers. The current model is that of a curved photoelectron wave emanating from the source atom and scattering from neighboring atoms; the

FT thus yields the path-length differences between the direct and scattered photoelectron waves.[5] Later studies have shown that the ARPEFS oscillations are dominated by atoms within a backscattering cone -- not just 180° backscattering. Hence, although the S 1*s* and S 2*p* ARPEFS data appear to be about 180° out of phase, the generality of the $(-1)^{\ell_i+1}$ factor for non-backscattering geometries is not established.

It is also important to ascertain whether these two ARPEFS data sets have the same frequencies and, therefore, the same peak positions in their FTs. Figure 1b compares the auto-regressive linear prediction (ARLP)-based FTs of the two $\chi(k)$ curves shown in figure 1a.[14] The ARPEFS-FTs from the 1*s* and 2*p* initial-states are, in fact, significantly different, contrasting expectations based on the earlier theory.[8]

First, Figure 1b shows the Generalized Ramsauer-Townsend (GRT) peak-splitting of the peak near 4Å in the 1*s* but not the 2*p* initial-state FT. Note that the GRT peak-splitting did not appear in the 1*s* initial-state FT in the early theory. The GRT splitting in the 1*s* initial-state ARPEFS-FT has been studied previously.[15] This splitting occurs because the scattering amplitude goes nearly to zero at a given angle and k, passing nearly through the origin in the complex plane and incurring a 180° phase shift. In the plane-wave approximation (PWA) used in the early theory, the atomic scattering factor, as described by

$$F_{PWA}(\theta_j, k) = \frac{1}{k}\sum_{\ell=0}^{\ell_{max}}(2\ell+1)e^{-i\delta_\ell}\sin(\delta_\ell)P_\ell(\cos\theta_j), \tag{1}$$

is independent of the final state. Here δ_ℓ is the ion-core partial-wave phase shift, $P_\ell(\cos\theta_j)$ is a Legendre polynomial, and θ_j denotes the scattering angle of a scattering atom j at a distance R_j from the source atom. It has been shown that the

PWA can only give approximate results in ARPEFS.[15,16] Because $F_{PWA}(\theta_j,k)$ is independent of the final state, the present work, which is based on differences between the final states, again illustrates the importance of using the curved-wave approximation (CWA) in ARPEFS to make accurate surface-structural determinations.

Barton and Shirley[16] discussed the CWA for the atomic scattering factor for an arbitrary initial state. Additional studies of the initial-state dependence of the atomic scattering factor have been completed for both photoelectron diffraction and extended x-ray absorption fine structure.[6,7,17-20] Based on the CWA, atomic scattering factors for an arbitrary initial state are described in ARPEFS by

$$F_{CWA}(\ell_f,\theta_j,k) \propto \frac{i^{\ell+1}kR_j}{e^{ikR_j}} h_\ell^+(kR_j) Y_{\ell_f m_i}(\hat{R}_j) F_{PWA}(\theta_j,k)\left(1+\frac{\ell(\ell+1)}{2ikR_j}\right) \quad (2)$$

where $h_\ell^+(kR_j)$ is the spherical Hankel function of the first kind and $Y_{\ell_f m_i}(\hat{R}_j)$ is the spherical harmonic evaluated at the angles given by the unit vector $\hat{R}_j$. Because F_{CWA} in Equation (2) is dependent on the final state, a given phenomenon, such as the GRT effect, may be present in the *p* final-state atomic scattering factor while at the same time being absent in the *s* or *d* final-state factor.

Figure 2 plots the final-state-dependent scattering factor in the complex plane. It is directly analogous to Figure 3 in Ref. 15. The scattering factors were calculated for θ_j=130.5° (the normal-emission scattering angle off the sulfur atom's four nearest-neighbor nickel atoms). The tick marks indicate the photoelectron wave-number scale in Å^{-1}. Each scattering factor curve is also labeled with its respective photoelectron final state. The (real part of the) scattering amplitude for a given k is the distance from the origin to that k-point on the scattering factor curve. The phase shift for a given k is given by the angle

between the positive real axis and that k-point on the scattering factor curve. For the *p* final state, the scattering amplitude is almost zero at $k \approx 7.5 Å^{-1}$ and the phase shift changes abruptly by 180°. Hence, a GRT effect in the S 1*s* initial-state ARPEFS data would be predicted from this curve, in agreement with experiment.

Turning to the S 2*p* ARPEFS case, there is also a significant dip in the scattering amplitude and a fairly abrupt 180° phase shift change for the *s*-wave scattering factor. However, the *d*-wave scattering amplitude varies modestly throughout the entire k range and even increases slightly at $k \approx 7 Å^{-1}$. Equally important, the *d*-wave scattering factor has no abrupt phase-shift changes. Thus no GRT effect would be possible for the *d*-wave alone. It will be shown that the final state in S 2*p* photoemission through this energy range is dominated by the *d*-wave and no GRT effect is predicted. The S 2*p* ARPEFS data and FT agree with this prediction as shown in Fig. 1.

The second way that the FTs in Fig. 1b differ is that the 6Å peak positions in the 1*s* and 2*p* initial-state ARPEFS-FTs are shifted. The shift is much smaller for the higher path-length difference (PLD) peak at 10 Å. These results are easily understood within the CWA formulation of atomic scattering factors. The peak positions in the ARPEFS-FTs are affected differently by the respective atomic scattering phase shifts depicted in Fig. 2. Furthermore, as R_j increases (larger PLD), the CWA approaches the PWA. The differences in the peak positions become smaller as the atomic scattering factor becomes less dependent on the final state. To test this interpretation, we computed FT curves from the theoretical MSSW best fits to the data and they reproduced the shifts shown in Fig. 1b.

The ARPEFS data and FT from the 2*p* initial state require both *s* and *d* partial waves to describe the final state. The interference between these two partial waves was examined theoretically for c(2x2)S/Ni(001) using the Kaduwela-Fadley MSSW code,[7] which is based on the scattering formalism of Rehr and Albers.[19]

Friedman and Fadley[21] have discussed this method and its application to photoelectron diffraction from arbitrary initial states.

For the calculations presented here, the radial dipole matrix elements, $R_{\ell_i \pm 1}$, and phase shifts, $\delta_{\ell_i \pm 1}$, were obtained from Goldberg *et al.*[22] These values describe the shape and phase relationship between the two partial waves, $\ell_i \pm 1$, and thus the true *s+d* final state. The scattering phase shifts for sulfur and nickel were provided by Kaduwela and Fadley.[23] Structural and non-structural parameters of c(2x2)S/Ni(001) were taken from previous ARPEFS studies.[6,7] The S-Ni interlayer spacing, $d_\perp$, is 1.30Å, and the first two nickel layers are separated by 1.86Å. The second-to-third nickel interlayer spacing is the bulk value, 1.76Å. Figure 3 compares the MSSW calculation to the experimental data. The agreement between theory and experiment is quite good.

The interference between the *s* and *d* partial waves was examined. Figure 4 compares the MSSW-ARPEFS curves calculated for the *s* and *d* partial waves, as well as for the actual *s+d* final state. The ratio of the S 2*p* radial dipole matrix elements, $\frac{R_{\ell_i+1}}{R_{\ell_i-1}}$, is greater than 3 throughout the ARPEFS energy range. Hence, in this particular case, we would expect the ARPEFS data to be dominated by the $\ell_i + 1$, or *d*, partial wave. To further this idea, we might be able to simulate the ARPEFS data to some reasonable level of accuracy by considering the *d* wave alone. This "$\ell_i + 1$ approximation" may be applicable more generally, but we shall investigate it here only for the S 2*p* case. In an ARPEFS study based on photoemission data from a non-*s* initial state, if the two partial waves in the final state give comparable contributions, then accurate information about both transition matrix elements, R_{ℓ_i+1} and R_{ℓ_i-1}, and their relative phase is required throughout the energy range to make accurate surface structural determinations. This information is available at various levels of approximation in the atomic photoemission theoretical literature.

On the other hand, if the ratio $\frac{R_{\ell_i+1}}{R_{\ell_i-1}}$ is large, it may be possible to analyze ARPEFS data to reasonable accuracy using contributions from only the single ℓ_i+1 partial wave. In this case, accurate information about the radial dipole matrix elements from the non-*s* initial states is not required. We have successfully tested this approach using the experimental S 2*p* ARPEFS data of c(2x2)S/Ni(001). Figure 5 shows the best fit of the experimental S 2*p* ARPEFS data with the MSSW calculations based on the actual *s+d* final state as well as the *d* partial wave alone. The quality of fit is measured by the R-factor, defined as:

$$R = \frac{\sum[\chi_e(k) - \chi_t(k)]^2}{\sum[\chi_e(k)]^2} \tag{3}$$

where $\chi_e(k)$ denotes the experimental ARPEFS data points, and $\chi_t(k)$ denotes the MSSW calculation based on either the *s+d* final state or on the *d* partial wave. By fitting with the complete *s+d* final state, the derived interlayer spacing between the adsorbate S layer and the first Ni substrate layer was $d_\perp$=1.31Å, in very good agreement with accepted value.[10] The R-factor value for this fit was 0.16, as shown in the inset in Fig. 5. By fitting over the same energy range with only the *d* partial wave, the values $d_\perp$=1.30Å and R=0.30 were obtained.

In summary, the final-state effects in the ARPEFS study of adsorbed surfaces were investigated using experimental S 1*s* and S 2*p* ARPEFS data from c(2x2)S/Ni(001). The experimental 1*s* and 2*p* ARPEFS data appear to be approximately 180° out of phase as predicted by an early theoretical description. However, FTs of the experimental 1*s* and 2*p* ARPEFS $\chi(k)$ data are quite different due to the curved-wave characteristics and the scattering-factor differences of the photoelectron final states. MSSW calculations were carrried out to study the final-

state effects. Based on the calculations, it was found for this particular case that the ARPEFS data from this S $2p$ non-s initial state can be analyzed using the $\ell_i + 1$ partial d-wave contribution alone. For this case, the ratio of the radial dipole matrix elements, $\frac{R_{\ell_i+1}}{R_{\ell_i-1}}$, is relatively large, exceeding 3 throughout the energy range. This approach may have wider applicablity for other core levels.

ACKNOWLEDGMENTS

The authors gratefully acknowledge Ajith Kaduwela and Chuck Fadley for use of their scattering code and phase shifts as well as many helpful discussions. This work was supported by the Director, Office of Energy Research, Office of Basic Energy Sciences, Chemical Sciences Division of the U.S. Department of Energy under Contract No. DE-AC03-76SF00098.

REFERENCES

[1]A. Liebsch, Phys. Rev. Lett. **32**, 1203 (1974);Phys. Rev. B **13**, 544 (1976).

[2]S. Kono, C.S. Fadley, N.F.T. Hall, and Z. Hussain, Phys. Rev. Lett. **41**, 117 (1978).

[3]D.P. Woodruff, D. Norman, B.W. Holland, N.V. Smith, H.H. Farrell, and M.M. Traum, Phys. Rev. Lett. **41**, 1130 (1978).

[4]S.D. Kevan, D.H. Rosenblatt, D. Denley, B.C. Lu. and D.A. Shirley, Phys. Rev. Lett. **41**, 1565 (1978).

[5]J.J. Barton, C.C. Bahr, Z. Hussain, S.W. Robey, J.G. Tobin, L.E. Klebanoff, and D.A. Shirley, Phys. Rev. Lett. **51**, 272 (1983).

[6]J.J. Barton, PhD Thesis, University of California, Berkeley, 94720 (1985)

[7]A. Kaduwela PhD Thesis, University of Hawaii at Manoa, Honolulu, Hawaii, 96822 (1991).

[8]S.Y. Tong and J.C. Tang, Phys. Rev. B **25**, 6526 (1982); J.C. Tang, Chin. Phys. Lett. **4**, 321 (1987).

[9]D.H. Rosenblatt, J.G. Tobin, M.G. Mason, R.F. Davis, S.D. Kevan, D.A. Shirley, C.H. Li, and S.Y. Tong, Phys. Rev. B **23**, 3828 (1981).

[10]J.J. Barton, C.C. Bahr, S.W. Robey, Z. Hussain, E. Umbach, and D.A. Shirley, Phys. Rev. B **34**, 3807 (1986).

[11]L.-Q. Wang, A.E. Schach von Wittenau, Z.G. Ji, L.S. Wang, Z.Q. Huang, and D.A. Shirley, Phys. Rev. B **44**, 1292 (1991); L.-Q. Wang, Z. Hussain, Z.Q. Huang, A.E. Schach von Wittenau, D.W. Lindle, and D.A. Shirley, Phys. Rev. B **44**, 13711 (1991).

[12]Z.Q. Huang, L.-Q. Wang, A.E. Schach von Wittenau, Z. Hussain, and D.A. Shirley, Phys. Rev. B **47**, 13626 (1993).

[13]Z.Q. Huang, Z. Hussain, W.T. Huff, E.J. Moler, and D.A. Shirley, Phys. Rev. B **48**, 1696 (1993).

[14]The ARLP based FT of the S 1*s* ARPEFS data presented here agrees with figure 6 in reference 10. In this work, the ARLP-FT has lower resolution because the S 1*s* data range was reduced to match the S 2*p* data range.

[15]J.J. Barton, Z. Hussain, and D.A. Shirley, Phys. Rev. B **35**, 933 (1987).

[16]J.J. Barton and D.A. Shirley, Phys. Rev. B **32**, 1892 (1985).

[17]A.G. McKale, G.S. Knapp, and S.-K. Chan, Phys. Rev. B **33**, 841 (1986); A.G. McKale, S.-K. Chan, B.W. Veal, A.P. Paulikas, and G.S. Knapp, J. De Pysique, Colloq. **47**, C8-55 (1986).

[18]A.G. McKale, B.W. Veal, A.P. Paulikas, S.-K. Chan, and G.S. Knapp, J. Am. Chem. Soc. **110**, 3763 (1988).

[19]J.J. Rehr and R.C. Albers, Phys. Rev. B **41**, 8139 (1990).

[20]J. Mustre de Leon, J.J. Rehr, C.R. Natoli, C.S. Fadley, and J. Osterwalder, Phys. Rev. B **39**, 5632 (1989); J. Mustre de Leon, J.J. Rehr, S.I. Zabinski, and R.C. Albers, Phys. Rev. B **44**, 4146 (1991).

[21]D.J. Friedman and C.S. Fadley, J. of Electron Spectroscopy and Related Phenomena **51**, 689 (1990).

[22]S.M. Goldberg, C.S. Fadley, and S. Kono, J. of Electron Spectroscopy and Related Phenomena **21**, 285 (1981).

[23]A. Kaduwela and C.S. Fadley, Private Communication.

FIGURES

Figure 1: a) Experimental S 1*s* (solid line) and S 2*p* (dotted line) ARPEFS data of c(2x2)S/Ni(001); b) ARLP based FT of the experimental S 1*s* (solid line) and S 2*p* (dotted line) ARPEFS data of c(2x2)S/Ni(001)

Figure 2: Final-state scattering factor calculations for *s* (dashed line), *p* (solid line), and *d* (dotted line) plotted in the complex plane (θ_j=130.5°). The tick marks indicate the photoelectron wave-number scale (Å^{-1}). The (real part of the) scattering amplitude for a given k is the distance from the origin to that k-point on the scattering factor curve. The phase shift for a given k is given by the angle between the real axis and that k-point on the scattering factor curve.

Figure 3: Comparison between the experimental S 2*p* ARPEFS data (solid line) and the MSSW calculation result (dotted line)

Figure 4: MSSW calculation results for the *s*+*d* final-state (solid line), the single *d* partial wave (dotted line), and the single *s* partial wave (dashed line)

Figure 5: Comparison between the experimental S 2*p* ARPEFS data (solid line) and the best fit MSSW calculation result based on the actual *s*+*d* final-state (dotted line) and the single *d* partial wave (dashed line); The inset shows the R-factor vs $d_\perp$ for the actual *s*+*d* final-state (solid squares) and the single *d* partial wave (open circles).

Figure 1: ARPEFS Experimental Data

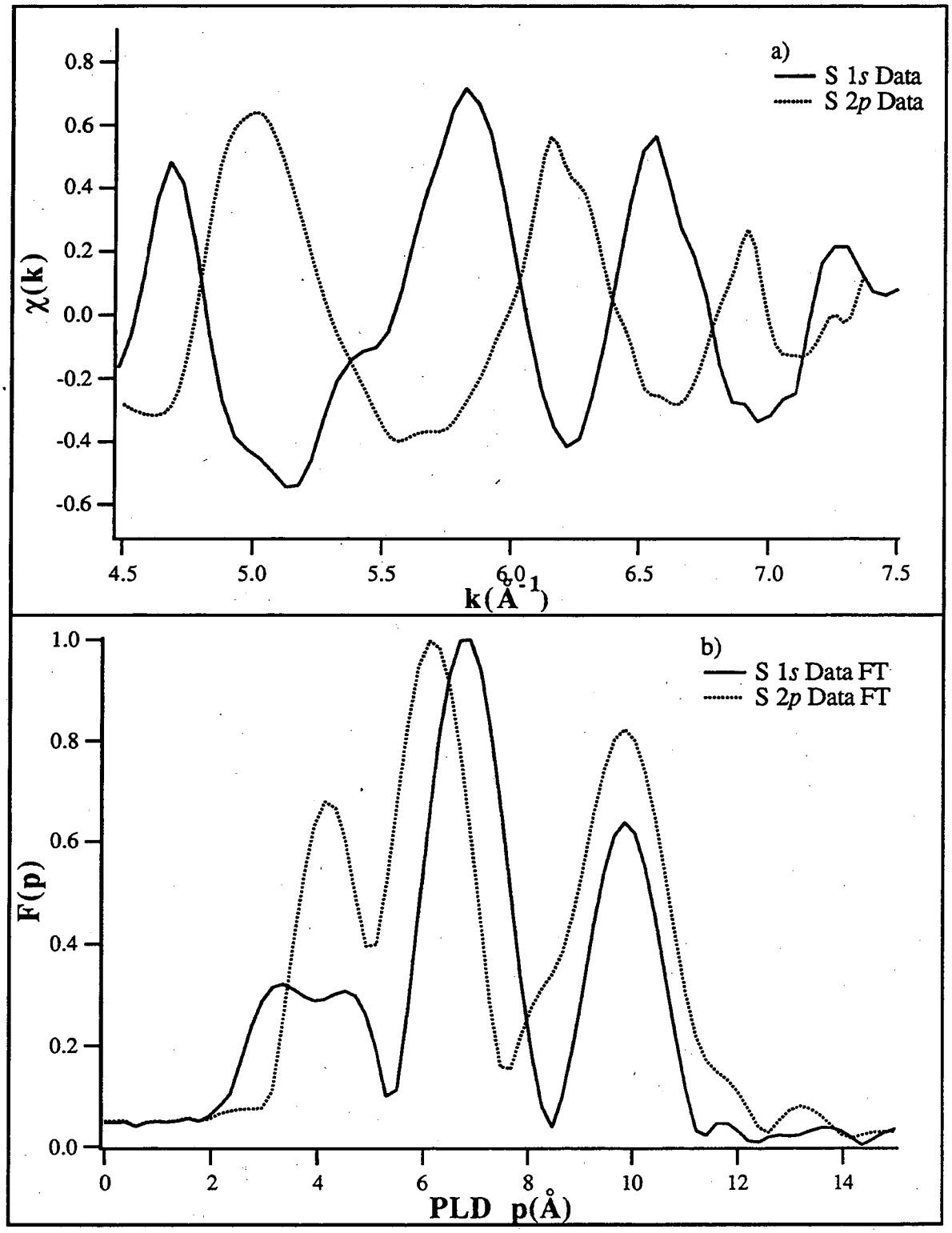

Figure 2: Final-State Scattering Factor Calculations
Plotted in the Complex Plane (θ_j=130.5°)

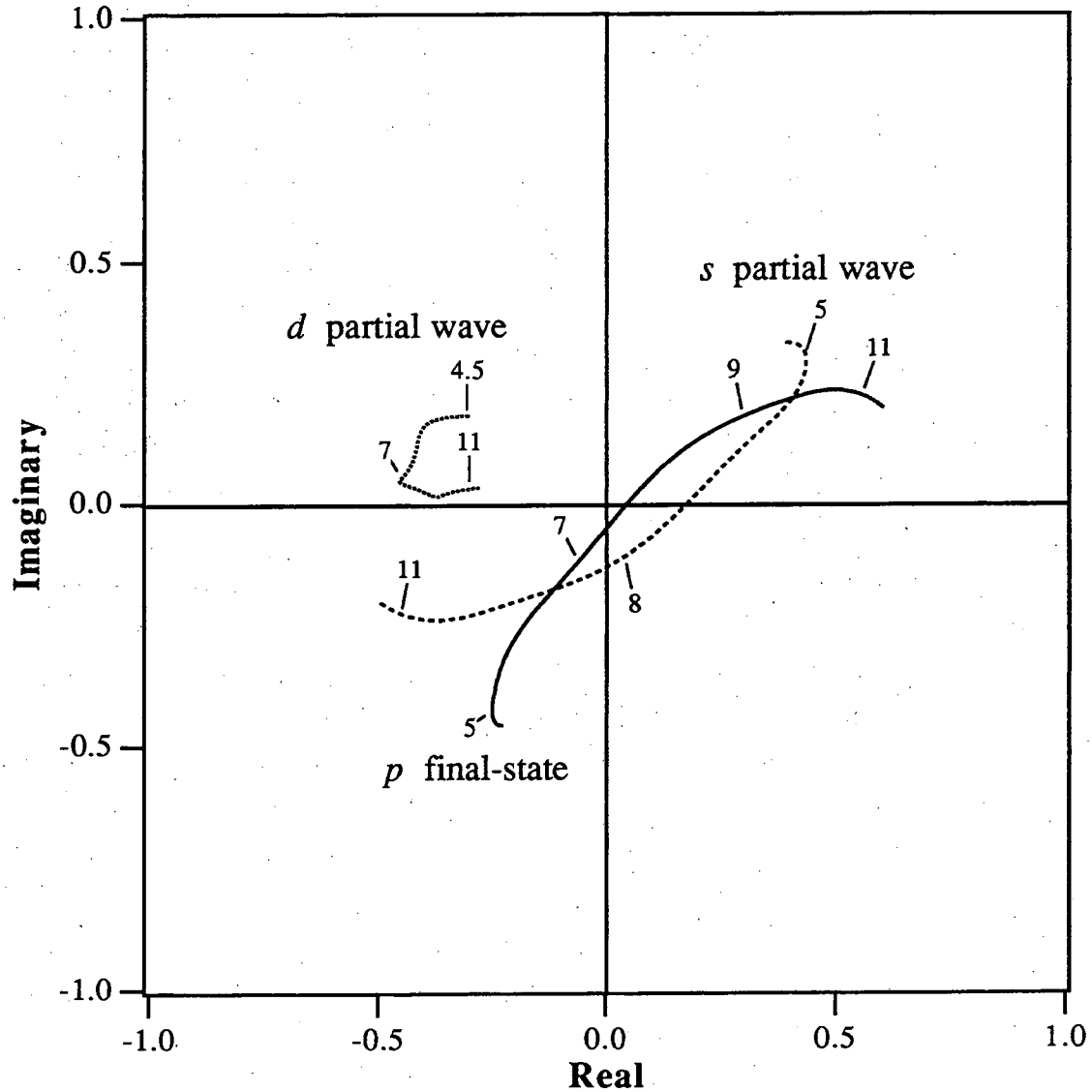

Figure 3: Experiment and MSSW Calculation (S 2*p* initial-state)

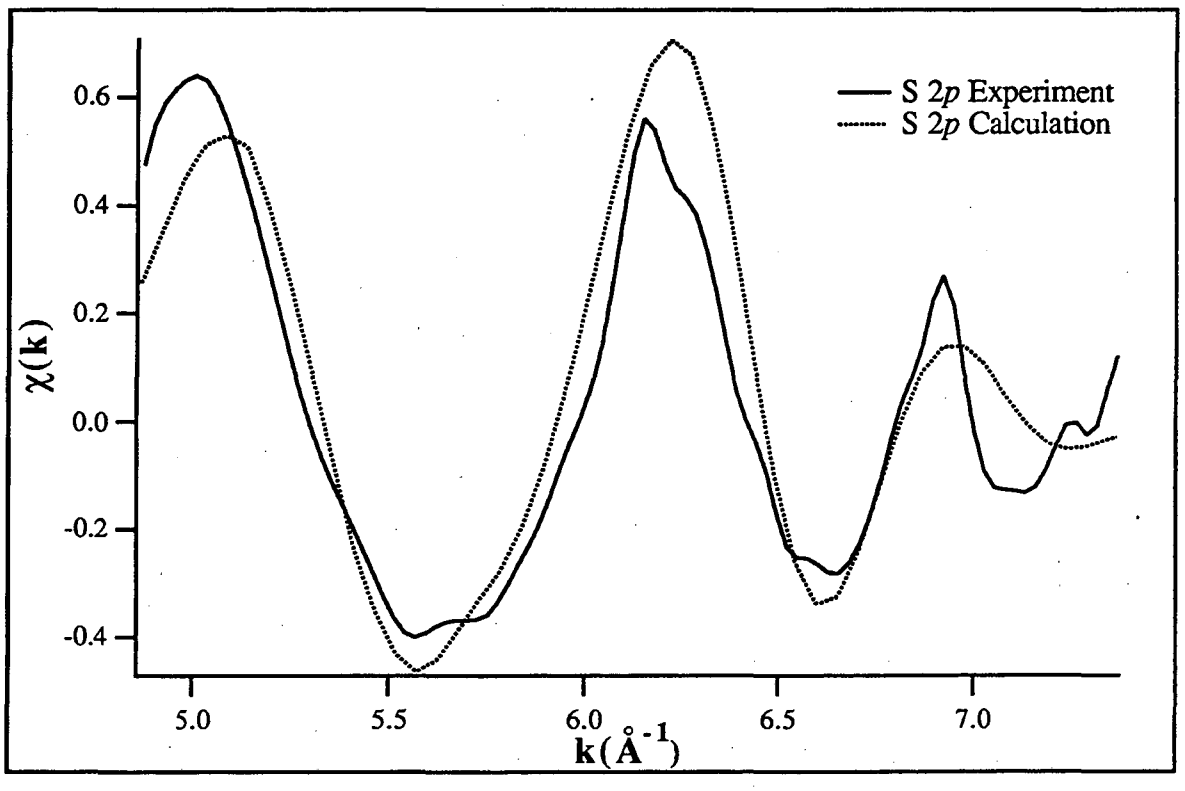

Figure 4: MSSW Calculations (S 2*p* initial-state)

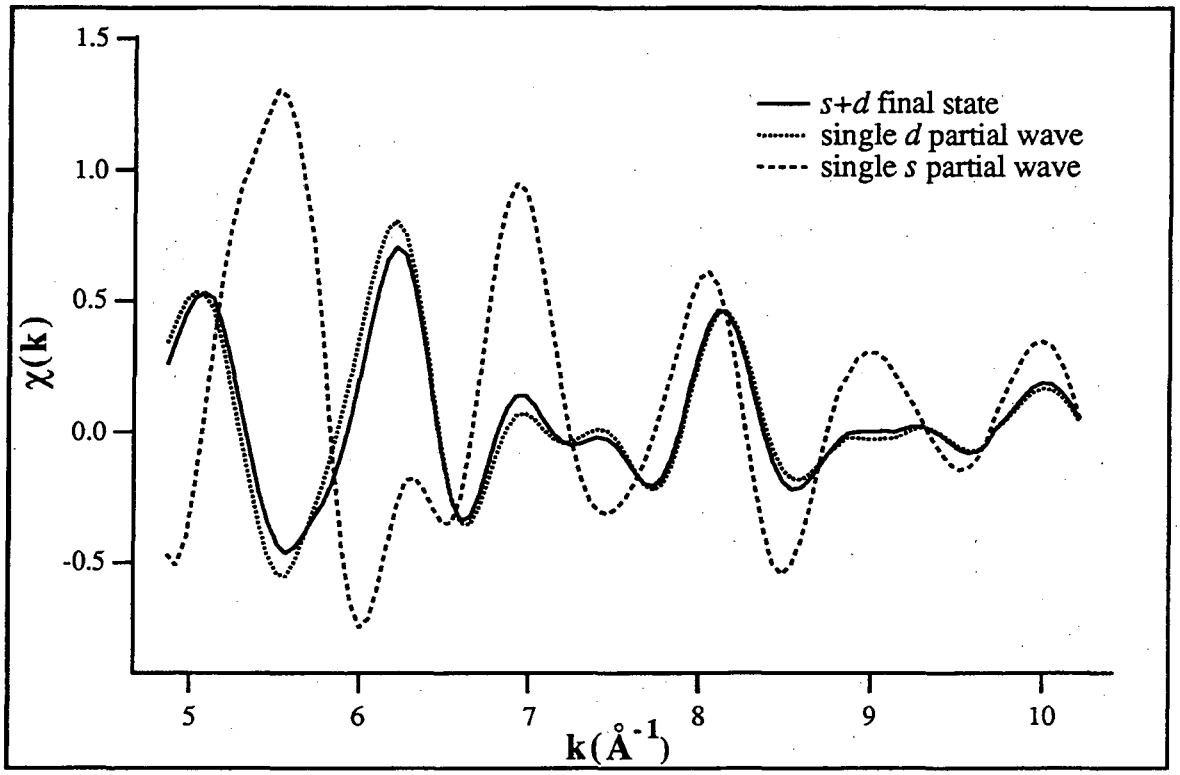

Figure 5: Experiment and MSSW Calculation (S 2*p* initial state):

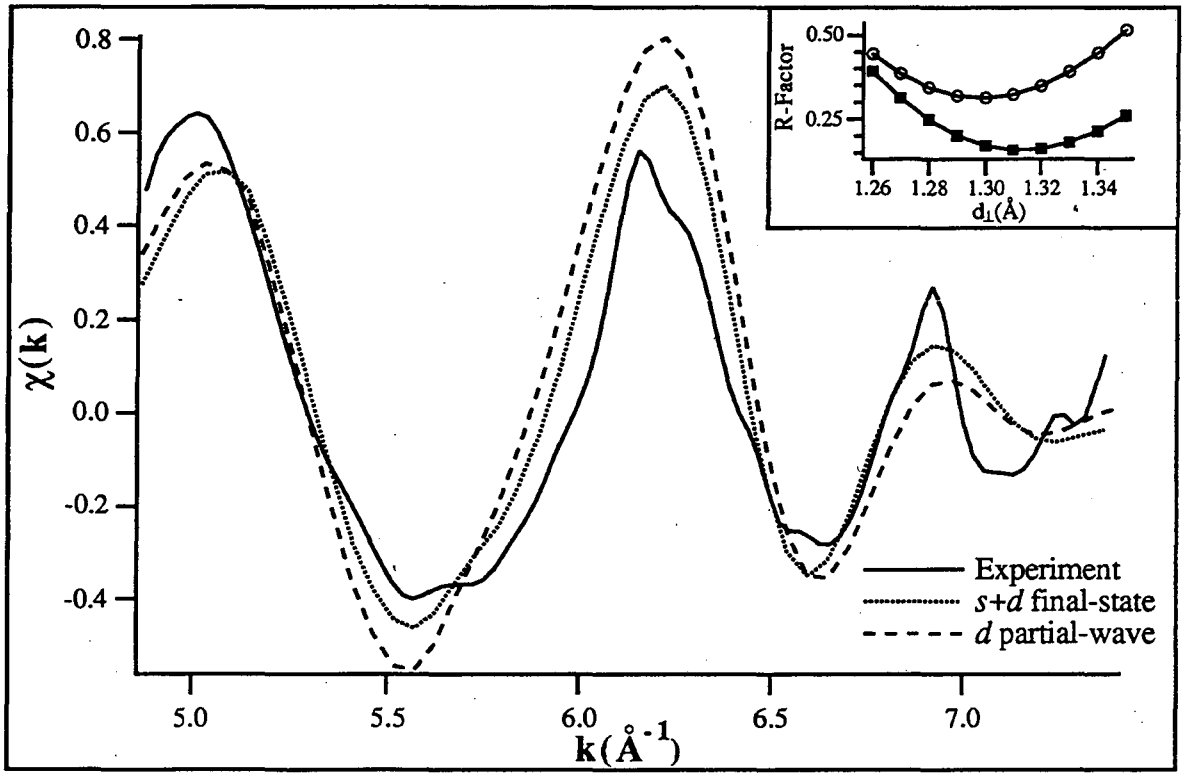

LAWRENCE BERKELEY LABORATORY
UNIVERSITY OF CALIFORNIA
TECHNICAL INFORMATION DEPARTMENT
BERKELEY, CALIFORNIA 94720

AAT227
LBL Libraries